Polymer 199 (2020) 122548

Contents lists available at ScienceDirect

Polymer

journal homepage: http://www.elsevier.com/locate/polymer

Crystal nucleation in poly(ether ether ketone)/carbon nanotube nanocomposites at high and low supercooling of the melt

Anne M. Gohn [a,b], Jiho Seo [c], Ralph H. Colby [c], Richard P. Schaake [d], René Androsch [b], Alicyn M. Rhoades [a,*]

[a] School of Engineering, Penn State Erie, 4701 College Drive, Erie, PA, 16563, United States
[b] Interdisciplinary Center for Transfer-oriented Research in Natural Sciences, Martin Luther University Halle-Wittenberg, 06099, Halle/Saale, Germany
[c] Department of Materials Science and Engineering, Penn State University, University Park, PA, 16802, United States
[d] SKF Research and Technology Development, 3992 AE, Houten, the Netherlands

ARTICLE INFO

Keywords:
PEEK
CNT
Nanocomposite
Nucleation
Crystallization
Fast scanning chip calorimetry

ABSTRACT

The engineering thermoplastic poly(ether ether ketone) (PEEK) has a rigid backbone that crystallizes relatively slowly upon cooling the melt. In this study, fast scanning chip calorimetry (FSC) was used to analyze isothermal crystallization between 170 and 285 °C, a range from about 27 K above the glass transition temperature up to the melting temperature. Incorporation of carbon nanotubes (CNT) enhances nucleation at all crystallization temperatures, including low temperatures. FSC also was employed to study crystallization at cooling rates spanning 0.33 to 8000 K/s, important as PEEK is subject to these conditions during melt processing. The critical cooling rate to produce a vitrified sample was increased from 500 K/s in the neat PEEK to 4000 K/s in a 5% CNT/PEEK nanocomposite due to faster nucleation rate caused by heterogeneous nucleation.

1. Introduction

The semi-crystalline thermoplastic poly(ether ether ketone) (PEEK) is often used in high-end engineering applications, such as medical, aerospace, automotive, and electrical, due to its mechanical performance and temperature resistance [1,2]. PEEK has a glass transition temperature (T_g) of about 145 °C and typically the melting temperature (T_m) is observed between 320 and 3655 °C [3]. The maximum rate of crystallization in neat PEEK is observed at 223 °C with a half-transition time of crystallization of approximately 0.4 s [3], with the rather low maximum crystallization rate, compared to other thermoplastics, related to its low chain mobility [4–9]. The crystal structure of PEEK is reported to be orthorhombic with unit cell parameters of a = 7.75 Å, b = 5.86 Å, and c = 10.00 Å, with the c-axis being parallel to the chain direction [10]. Absolute crystallinity ranges of 30–42% have been reported in commercial neat PEEK systems, dependent on the mass-average molecular weight (M_w) (26,100 g/mol < M_w < 44,300 g/mol) [3].

The use of carbon nanotubes (CNT) in polymer composites has been widely studied in recent years due to their ability to greatly improve properties even at low loading [11–14]. CNT/polymer nanocomposite enhanced properties paired with a low percolation threshold [15–21] makes them an ideal candidate for industries such as electrical [15,20], textile [22–24], coatings [25,26], aerospace [27–29], and biotechnology [30–32]. Multi-walled carbon nanotubes (MWCNT) can have differing dimensions based on an outside diameter ranging from 2 to 30 nm and a length of 0.5–50 μm, yielding a range of aspect ratios from 33 to over 3000 [33–35]. The high aspect ratio provides a high specific surface area, ranging from 50 to 1300 m^2/g [36]. It is due to these high surface areas that the CNT composites are able to form a percolation network at low loading levels [15,37,38].

The crystallization behavior of PEEK/CNT nanocomposites has been studied with conflicting findings. Though researchers found that CNTs act as heterogeneous nucleators in other polymer systems [39–41], the crystallization behavior of PEEK has mixed reports. Rong and coworkers found that increasing content of unmodified MWCNTs up to 5 wt % elevated the crystallization temperature (T_c) on cooling, indicating a heterogeneous nucleation effect [42]. In contrast, Díez-Pascual reported that the use of single-walled carbon nanotubes (SWCNT) in PEEK decreased T_c due to a confinement effect, with restricted mobility of the polymer chains [43]. Otherwise, there is agreement that the use of CNTs does not affect the crystal structure [43]. PEEK nanocomposites

* Corresponding author.
E-mail address: amh234@psu.edu (A.M. Rhoades).

https://doi.org/10.1016/j.polymer.2020.122548
Received 14 February 2020; Received in revised form 18 April 2020; Accepted 1 May 2020
Available online 5 May 2020
0032-3861/

containing fillers with particulate geometry have been studied by the use of alumina nanoparticles, and it was found that though the nucleation rate was increased, slower growth was observed due to reduced chain mobility and earlier spherulite impingement [44]. A heterogeneous nucleating effect has also been shown to occur in PEEK through flow induced crystallization, where molecular orientation has decreased the crystallization time under isothermal crystallization conditions [45].

An increased mechanical response of CNT nanocomposites is also valuable in engineering applications. Specifically when employed in PEEK systems, it was found that 15 wt-% CNTs increased Young's modulus 98% and the ultimate tensile stress 14% [46]. At 4 wt % loading, the flexural strength was increased by 15.5% [35]. PEEK/CNT nanocomposites were also found to increase transfer-film coverage in tribological applications [47]. The mechanical, thermal, and tribological properties are also dependent on the microstructure developed during solidification from the molten state, specifically in the case of injection molded engineering applications [48–50].

Fast scanning chip calorimetry (FSC) is a necessary tool to establish crystallization at high supercooling [3,9,51]. The current available literature on PEEK nanocomposite crystallization covers only low cooling rates (up to 20 K/min) and high temperatures (>292 °C). In other polymers, such as polyamides 6, 11, and 12, nucleation in nanocomposites has been studied using FSC across the temperature window spanning temperatures close to T_g and T_m in order to analyze crystallization at process-relevant rates and temperatures (up to 4000 K/s) [52–55]. This study is the first attempt to employ FSC to investigate nanocomposites of PEEK and to learn more about the heterogeneous nucleation behavior in this complex system.

2. Experimental

2.1. Material

A PEEK/carbon nanotube masterbatch at 15 wt % loading was purchased from Hyperion Catalysis (MB 9015–00). The CNT diameter, length, and specific surface area are 10 nm, 10 μm, and approximately 200 m^2/g, respectively [56]. For the purpose of diluting the masterbatch, PEEK grade 150G was purchased from Victrex. The glass transition temperature at zero heating rate, the equilibrium melting temperature, number-average molar mass (M_n) and weight-average molecular mass (M_w) are around 142 °C, 380 °C, 10,000 g/mol and 26,100 g/mol, respectively [3]. The bulk enthalpy of melting PEEK has been reported to be 130 J/g [10]. Melt mixing of the neat resin with the masterbatch was performed on an Intelli-Torque Plasti-Corder from CW Brabender equipped with a 19 mm diameter screw and a 30:1 L/D ratio. Prior to extrusion, PEEK materials were dried overnight at 120 °C to rid the polymer of any moisture. The pelletized masterbatch was then mixed with neat PEEK to produce 1, 2, 5, and 10 wt-% PEEK/CNT nanocomposites by extrusion at 50 RPM. Temperatures were staggered at 355/360/370/375 °C from feed zone to nozzle. Once extruded from the die, the molten strand was cooled in a water bath and pelletized. As a reference material, the neat PEEK was also extruded at the same conditions as the CNT composites in order to have a baseline that has a consistent thermal history.

2.2. Instrumentation

2.2.1. Differential scanning calorimetry (DSC)

A standard DSC1 from Mettler-Toledo was used to collect information regarding crystallization at low cooling rates. Cooling was controlled with a Thermo Scientific EK90/MT intracooler. A sample of approximately 6 mg was heated at a rate of 10 K/min to 400 °C. The sample was then cooled at 5, 10, 20, and 30 K/min in a consecutive loop using the consistent heating rate between segments. A nitrogen purge was applied at 30 mL/min.

2.2.2. Fast scanning chip calorimetry (FSC)

Crystallization was studied with a power-compensating Mettler-Toledo Flash DSC 1 cooled with a Huber intracooler TC100. Sample sensors were conditioned and temperature-corrected prior to performing any experiments. To minimize sample oxidation and prevent atmospheric moisture in the sample chamber, the test chamber was purged with ultra-high purity nitrogen gas at a flow rate of 60 mL/min. FSC samples were prepared by microtoming the extruded pellets to 12 μm thickness and cutting laterally with a scalpel under a microscope to achieve approximately a 75 μm × 75 μm square specimen. A thin layer of Wacker AK 60,000 silicon oil was applied between the sample and sensor membrane to improve THE thermal contact. To remove any shear history in the extruded pellets, the FSC samples were first heated to 400 °C for 5 s before the experiments were conducted.

Fig. 1 displays images of the FSC methods used in this work. Fig. 1a displays the non-isothermal crystallization method, where the sample was heated to 380 °C, followed by cooling at a specified rate between 0.33 and 8000 K/s to −60 °C. A subsequent heating scan of 500 K/s was then used to analyze the crystalline fraction developed during the previous cooling step. This process was repeated with the same sample until all cooling rates were analyzed. Multiple scans were repeated for consistency to confirm that no sample degradation occurred during the sequential thermal analysis methods. The isothermal crystallization method is shown in Fig. 1b. A single sample was used in series to analyze all crystallization temperatures ranging from 170 to 285 °C. The sample was heated to 380 °C, quenched at 5000 K/s to the desired isothermal

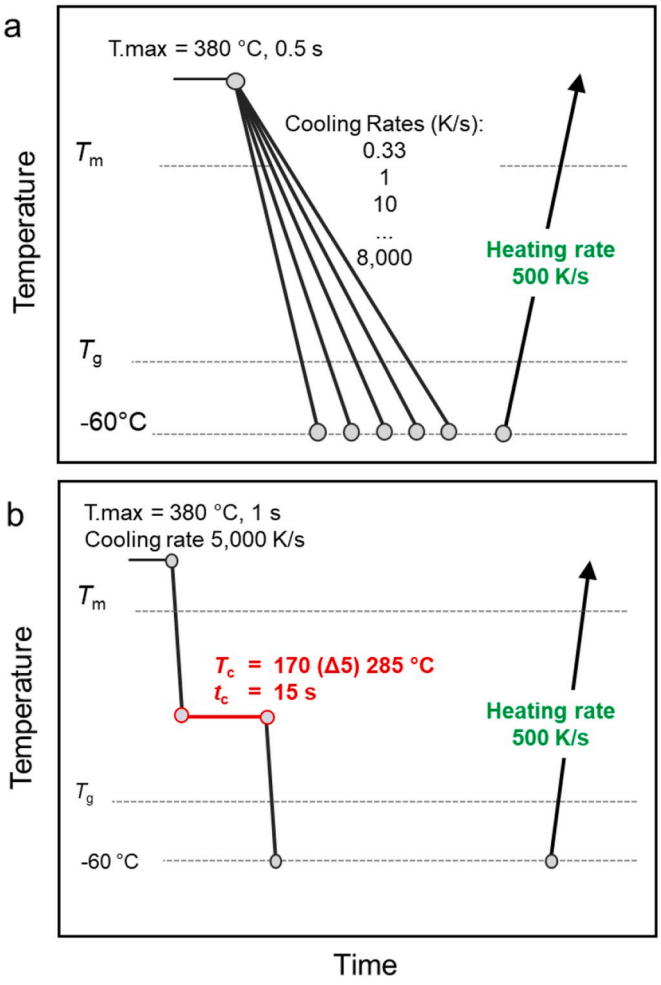

Fig. 1. Time-temperature protocols for FSC analysis: (a) non-isothermal crystallization at cooling rates from 0.33 to 8000 K/s; (b) isothermal crystallization ranging from 170 to 285 °C.

crystallization temperature, where it was held for up to 15 s to allow for complete crystallization. After the crystallization step, it was quenched to below T_g, followed by a heating segment back to the melt. This process was repeated with the same sample until all crystallization temperatures were analyzed.

2.2.3. Polarized-light optical microscopy (POM)

The samples were imaged employing a Leica DM750P microscope and DMC2900 camera. The samples were conditioned on the FSC sensor under specific crystallization conditions. The sensor was removed from the FSC unit and imaged in reflection mode with the sample and sensor between crossed polarizers.

2.2.4. Atomic force microscopy (AFM)

AFM measurements were performed using a Bruker Dimension Icon. Samples were conditioned isothermally at 185, 250, or 290 °C on the FSC chip without an oil layer before being quenched to room temperature. The stainless-steel AFM specimen disc was prepared with double-sided adhesive tape, and the pre-conditioned polymer sample attached to the sensor membrane was adhered to the sample disc. PeakForce tapping imaging mode was used with a ScanAsyst Air Probe (0.4 N/m spring constant), and image analysis was done using Nanoscope Analysis software.

3. Results and discussion

3.1. Standard DSC non-isothermal crystallization

Non-isothermal crystallization was studied through standard DSC at cooling rates of 5, 10, 20, and 30 K/min. The cooling traces associated with the neat PEEK and 10 wt-% CNT-filled PEEK are displayed in Fig. 2. It is shown that the crystallization of the nanocomposite initiates at a higher temperature than that of the neat PEEK, and that the peak crystallization temperature (T_c) is higher than that of the unmodified PEEK resin. The broader crystallization peak in the nanocomposite also implies a slower growth rate. To summarize the standard DSC data for all composites, Table 1 displays the peak crystallization temperature (T_c), the enthalpy of crystallization per polymer fraction (ΔH_c), the crystallinity developed on cooling (X_c), and the subsequently recorded melting peak temperature (T_m) of the non-isothermally formed crystals. It is evident that the inclusion of CNTs in the system slightly increases T_c, indicating that the CNTs are acting as heterogeneous nucleators and even yield a slightly higher degree of crystallinity than the neat PEEK. In studying the melting temperature of these materials, a slight decrease in T_m is observed with increasing cooling rate, indicating a lower degree of crystal perfection/size, in both neat PEEK as well as the nanocomposite. This indicates that the inclusion of CNTs does not change the stability of the crystals formed on cooling.

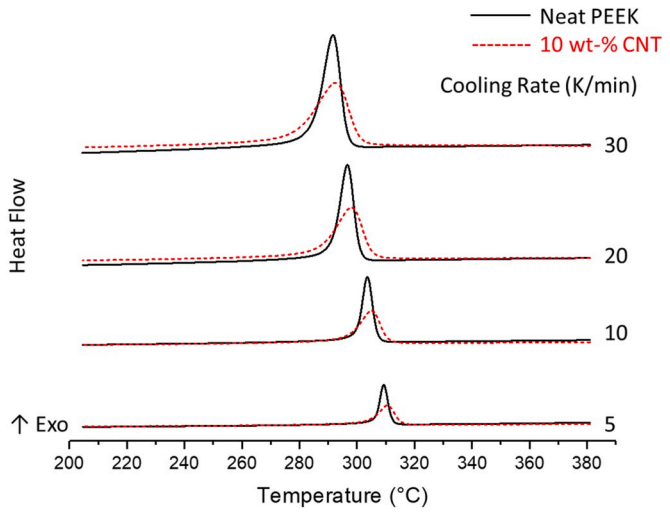

Fig. 2. Standard DSC cooling curves of neat PEEK (black, solid) and 10 wt-% CNT/PEEK composite (red dashed) at the cooling rates of 5, 10, 20, and 30 K/min. Curves have been normalized to sample mass. The onset and peak crystallization temperature of 10 wt-% CNT/PEEK composites are higher than in neat PEEK for all cooling rates. (For interpretation of the references to colour in this figure legend, the reader is referred to the Web version of this article.)

Table 1
Standard DSC data on PEEK/CNT nanocomposites.

Sample	Cooling Rate (K/min)	T_m (°C)	T_c (°C)	ΔH_c (J/g)	X_c (%)
Neat PEEK	5	345.5	309.0	48.7	37.5
	10	344.5	303.4	46.0	35.4
	20	343.9	296.5	43.3	33.3
	30	343.5	291.6	42.2	32.5
1 wt-% CNT	5	345.5	310.1	54.5	41.9
	10	344.7	304.8	51.1	39.3
	20	343.9	298.3	47.6	36.6
	30	343.1	293.2	44.9	34.5
2 wt-% CNT	5	344.7	311.1	52.9	40.7
	10	343.9	305.6	49.4	38.0
	20	343.1	299.3	46.8	36.0
	30	342.7	294.9	45.3	34.8
5 wt-% CNT	5	345.3	311.7	50.7	38.4
	10	344.1	306.6	47.2	37.5
	20	343.1	300.7	40.9	36.5
	30	342.9	296.5	44.7	34.3
10 wt-% CNT	5	345.1	310.3	58.7	45.2
	10	344.1	305.0	56.1	43.1
	20	343.1	298.1	55.0	42.3
	30	342.9	293.0	54.2	41.7

3.2. Non-isothermal crystallization of PEEK/CNT nanocomposites

An FSC-cooling-rate analysis was performed to find the critical cooling rate for quenching, above which crystallization is completely supressed on cooling to below T_g. In this experiment, as depicted in Fig. 1a, the sample is heated to 380 °C, where it is held for 0.5 s. It is then cooled at a specific rate between 0.33 and 8000 K/s. A constant heating rate of 500 K/s was used to analyze the fraction of crystals produced on cooling via their enthalpy of melting. The relative enthalpy of melting for each sample was then calculated with regard to the maximum enthalpy of melting produced at the lowest cooling rate. The enthalpy of melting normalized to a maximum relative crystallinity at the lowest cooling rate is displayed as a function of the cooling rate in Fig. 3.

The neat PEEK was found to have a critical cooling rate of 500 K/s. Beyond the critical cooling rate of 500 K/s, FSC can not detect any melting peaks on the subsequent heating at 500 K/s implying that no crystallization occurs during the cooling. With the addition of 1 and 2 wt-% CNTs, the critical cooling rate increases to ~1000 K/s. At high loadings of 5 and 10 wt-%, the critical cooling rate is further increased to ~4000 K/s. On an application note, it is known that in injection molding manufacturing processes, polymers may experience cooling rates higher than 600 K/s when the molten material meets the cold steel mold wall [57]. With the addition of CNTs into the PEEK matrix, it can be expected that the crystalline fraction developed in-mold during part manufacturing is increased, potentially reducing post-process annealing and issues related to low crystallinity.

3.3. Isothermal crystallization of PEEK/CNT composites

Isothermal crystallization times of neat PEEK has been reported using FSC [3,51], and the findings in this work have good agreement with published results. The peak time of crystallization as a function of temperature (Fig. 4) shows a unimodal distribution with a minimum crystallization time of 0.77 s at 225 °C. The addition of CNTs reduces the

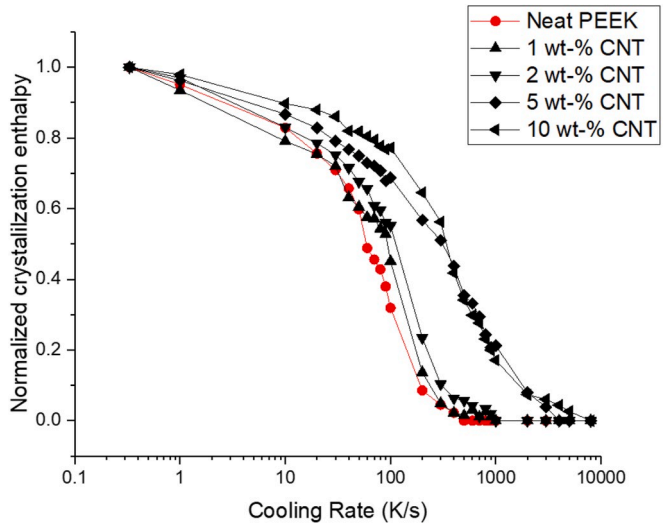

Fig. 3. The normalized crystallinity as a function of cooling rate from 0.33 to 8000 K/s for neat PEEK and PEEK/CNT composites normalized to the enthalpy at the lowest cooling rate of 0.3 K/s.

peak time of crystallization due to the availability of additional heterogeneous nucleation sites. The peak time decreases with increasing content of CNT, but at a loading above 5 wt-%, the nucleating effect has reached its saturation limit, likely due to aggregation of the nanofiller [58]. At 5 and 10 wt-% loading levels, a signal can only be obtained at temperatures between 245 and 285 °C. At temperatures below 245 °C, crystallization is too fast to be detected with the FSC employed in this study. It is known that the crystallization event is occurring during the isothermal step, even though a signal cannot be obtained, because the subsequent heating traces show that the melting of the "original melting peak," indicative of the crystallization temperature [59], is following the melting pattern associated with crystallization at each temperature. This behavior is shown in Fig. S2 in the Supporting Information document.

The nucleating efficiency of the CNT can be quantified through an acceleration factor (ε) evaluated by changes in crystallization rate (r_c), or peak-time of crystallization (t_p), to be calculated as [60] :

$$\varepsilon = \frac{r_c(\alpha_{CNT})}{r_c(\alpha_{CNT}=0)} \cong \frac{t_p(\alpha_{CNT}=0)}{t_p(\alpha_{CNT})} \quad (1)$$

If the ratio ε yields an acceleration factor of 1 , no nucleation advantage is gained from the CNT additive. With increasing ε, the system displays increasing nucleating efficiency. Fig. 5 indicates that all CNT nanocomposites exhibit an acceleration factor greater than 1, and that the acceleration factor increases with increasing CNT content and with decreasing crystallization temperature, the latter indicating that heterogeneous nucleating activity is more enhanced as the mobility of polymer-chain segments decreases. In other works on PP/CNT systems, at low CNT loadings (<5%), the acceleration factor increased with decreasing temperature through the heterogeneous nucleating regime, but slowly converged to a value of 1 in the homogeneous nucleation regime. This behavior was exaggerated at high CNT contents (5%), where the acceleration factor displayed an increasing trend to the exact shift in heterogeneous/homogeneous nucleation mechanism displayed by an abrupt drop in acceleration factor from approximately a value of 9 to 1 [60]. In comparison, the PEEK nanocomposite acceleration factor never converges to a value of 1 at low temperatures, indicating that the system maintains heterogeneous nucleation throughout the full temperature window studied.

In a study evaluating cold crystallization of semi-rigid polymers, Nogales and coworkers studied PEEK using X-ray scattering and dielectric spectroscopy simultaneously. They found that the induction time for PEEK' crystallization is controlled by low segmental mobility, causing slow development of the pre-crystalline nanostructures, or self-seeding [61]. By introducing a favorable heterogeneous nucleating material, such as CNT, the nucleation process that Nogales found to be prohibitory to PEEK's crystallization can be reduced dramatically, as shown by a reduction in crystallization time. The heterogeneous nucleating behavior documented in PEEK systems has to date only been studied at low supercooling where nucleation effects are pronounced [42–45]. This study also evaluates the nucleating efficiency at high supercooling, which is often the case under manufacturing conditions. The experiments designed in this study reveal the seemingly heterogeneous nucleating behavior of PEEK/CNT nanocomposites at high supercooling.

In previous studies of isothermal crystallization performed on nanocomposites, crystallization was only affected in the heterogeneous nucleation regime [52–54], including studies of CNT nucleation in poly (ε-caprolactone) (PCL) [58], poly(ethylene terephthalate) (PET) and

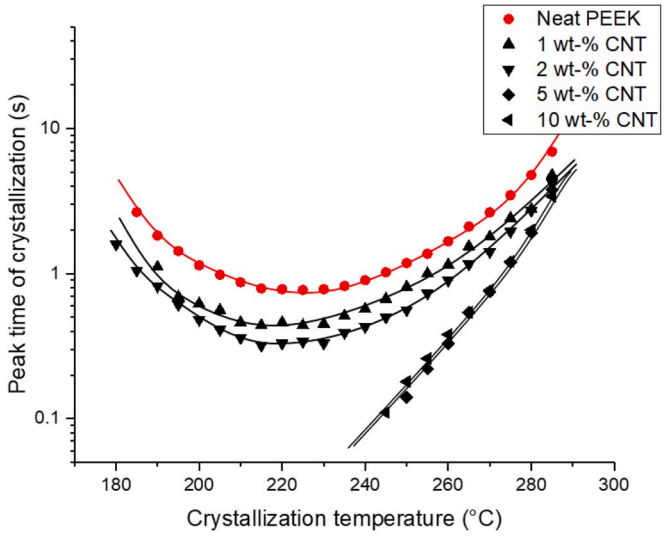

Fig. 4. Peak-time of crystallization of neat PEEK and PEEK/CNT composites between 180 and 285 °C. For 5 and 10 wt-% CNT/PEEK composites, the crystallization peak times cannot be monitored below 245 °C due to too high crystallization rates. The lines are a guide for the eye.

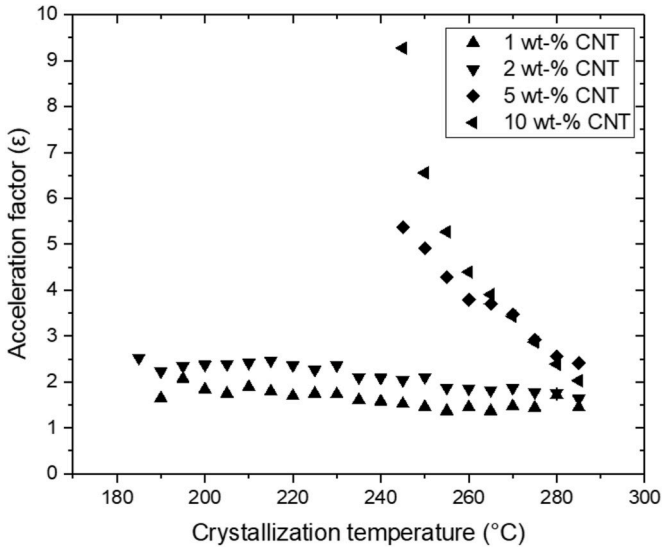

Fig. 5. Acceleration factor as a function of crystallization temperature for PEEK/CNT composites.

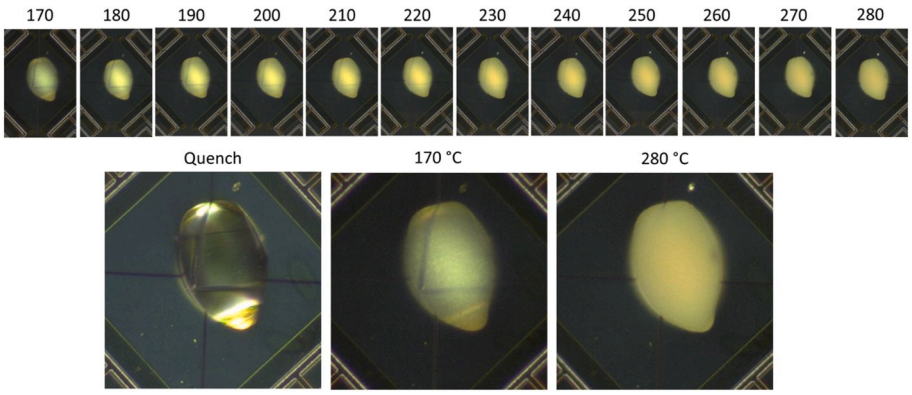

Fig. 6. Appearance of neat 150G PEEK in polarized-light optical microscopy at crystallization temperatures ranging from 170 to 280 °C, including a quenched (visibly amorphous) reference.

poly(butylene terephthalate) (PBT) [62]. PCL and PET are of most interest in comparison due to their similar isothermal crystallization behavior where a single minimum in the half-time curve is observed. At low temperatures, regardless of nanofiller concentration, PCL and PET peak-times of crystallization are unaffected, indicating homogeneous nucleation. This convergence of half time of crystallization at low temperature helps to distinguish a transition between homogeneous and heterogeneous nucleation. However, PEEK/CNT never converged to the neat system at low temperatures since heterogeneous nucleation was dominant in all crystallization temperatures ranging from 170 to 285 °C performed in this study.

POM and AFM are often used to identify homogeneous and heterogeneous nucleation because the resulting superstructures and crystal morphologies are largely different [4,5]. As for example reported in previous studies on polyamide 66 (PA 66), high-temperature crystallization via heterogeneous nucleation produces large, spherulitic superstructures and lamellar crystals while on low-temperature crystallization, where homogeneous nucleation occurs, nodular crystals with a superstructure not detectable by POM develop [5]. Fig. 6 shows POM micrographs of neat PEEK samples isothermally crystallized at temperatures ranging from 170 to 280 °C. Similar to the isothermal crystallization method shown in Fig. 1b, the PEEK was heated to 380 °C, held at this temperature for 1 s, and then quenched at 5000 K/s to the target crystallization temperature to allow for crystallization for 30 s. The sample was then further quenched to room temperature, where the FSC chip was taken out of the calorimeter and observed by POM. As a reference, a sample was also examined after quenching to room temperature at 5000 K/s from 380 °C, producing a fully amorphous sample. It has been found in PA 66 and PBT, which both display a bimodal temperature-dependence of the peak-time of crystallization, that the POM micrographs of FSC samples transition from transparent/non-birefringent in the homogeneous nucleation regime to opaque/birefringent in the heterogeneous nucleation regime [4,5]. However, the PEEK sample does not show such behavior since low-temperature crystallization still is connected with opacity of the sample, indicating presence of larger heterogeneities.

To explore the fading opacity of the samples when decreasing the crystallization temperature, the degree of crystallinity was analyzed via the enthalpy of melting in the subsequent heating scan after isothermal crystallization, shown in Fig. 7 together with the peak time of crystallization as a function of crystallization temperature. As crystallization temperature increases, the melting enthalpy increases as well, indicating that a higher degree of crystallization is achieved at higher temperatures.

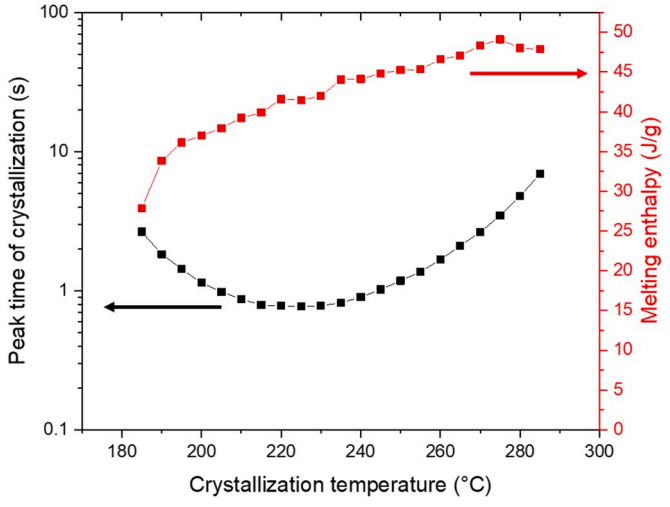

Fig. 7. Melting enthalpy as a function of the temperature of previous isothermal crystallization (right) and peak time of crystallization as a function of isothermal crystallization temperature (left).

3.4. Morphology of PEEK/CNT nanocomposites

In an effort to evaluate the microstructure and further investigate the result of unexpected crystallization behavior at low temperatures, AFM was employed. Samples of neat PEEK, and PEEK containing 2 wt-% CNT and 5 wt-% CNT were chosen as representative samples from the range of loading levels. Three crystallization temperatures spanning the range from T_g to T_m were chosen for this analysis, namely, 185, 250, and 290 °C.

Fig. 8 shows the AFM images for neat PEEK crystallized at 290 °C in both error mode (top row) and height mode (bottom row). Samples are organized by column with increasing magnification from left to right. The neat PEEK shows spherulites of about 1–2 μm in diameter, and presence of lamellae with a thickness of about 17.5 ± 4 nm.

A matrix of images obtained on neat PEEK and nanocomposites containing 2 and 5 wt-% CNT crystallized at 185 °C, 250 °C, and 290 °C is displayed in Fig. 9. All images presented here are shown in error mode due to high topographical detail. The scale bar for all images is shown in the upper right image. In the neat PEEK, as the crystallization temperature is decreased from 290 to 185 °C, the spherulitic superstructure is preserved. However, the spherulite size strongly decreases to submicron level, and the lamellae appear more densely packed together. A similar behavior is observed in the 2 wt-% CNT nanocomposite. At a 5 wt-% loading of CNTs, crystallization at 290 °C also displays a spherulitic microstructure like the other samples, but the nuclei density is increased. The neat PEEK and 2 and 5 wt-% CNT nanocomposite display some radial growth at 185 °C which corroboratescalorimetric results, indicating that there is some heterogeneous nucleation present at low

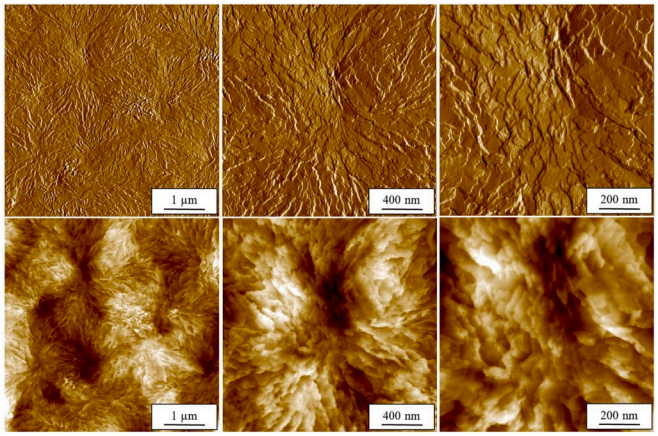

Fig. 8. AFM images of neat PEEK crystallized at 290 °C for 300 s. Top row images display error mode and the bottom row images display height mode. The images were taken from the same sample with increasing magnification from left to right.

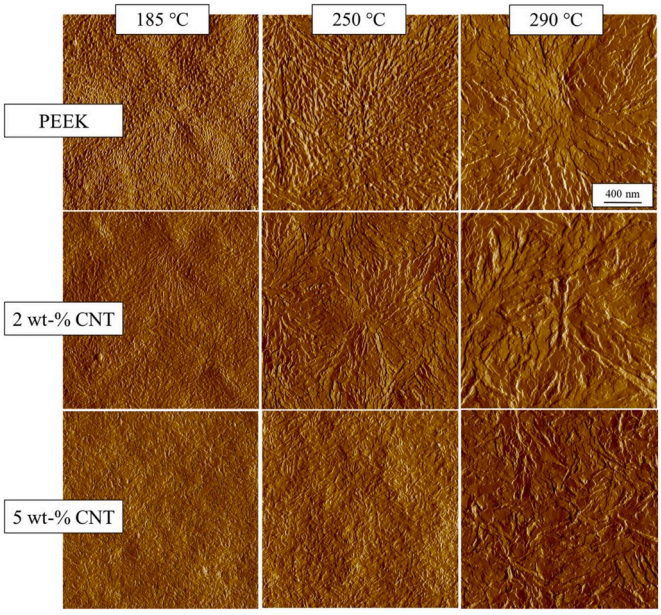

Fig. 9. AFM error mode images captured for neat PEEK (top row), and PEEK with 2 wt-% CNT (middle row) and 5 wt-% CNT (bottom row), isothermally crystallized at 185 °C (left column), 250 °C (middle column), and 290 °C (right column).

temperatures. This behavior has been confirmed with multiple samples. In previous works by Ivanov et al., spherulitic structures were also observed in PEEK at low crystallization temperature (<190 °C) when cold crystallizing after a quench from the melt [63,64]. This growth is similar to the melt crystallization displayed Fig. 9, as heterogeneous nucleation sites are developed during the fast quench to below T_g.

4. Conclusions

PEEK/CNT nanocomposites were analyzed for their crystallization behavior at a range of non-isothermal rates and isothermally at high and low supercooling of the melt. It was found that the CNTs nucleated the PEEK system at all temperatures tested between 170 and 280 °C, which indicates heterogeneous crystallization dominates at the full temperature spectrum analyzed here. An analysis of the acceleration factor (ε) evaluated by changes in crystallization rate peak-time of crystallization (t_p) showed that the heterogeneous nucleating effect was stronger with decreasing temperature. POM of isothermally crystallized samples indicates that at all temperatures, structural heterogeneities are large enough to be detected by visible light, which indicates microstructure and heterogeneities of the order of magnitude larger than half a micron. AFM confirms that there is heterogenous nucleation occurring at low crystallization temperatures observed by radial growth. Standard DSC results show that CNTs heterogeneously nucleate PEEK, though also slowing growth.

Non-isothermal crystallization as studied by FSC shows that the critical cooling rate can be increased from 500 K/s in the neat PEEK to 4000 K/s in a highly loaded (5%) CNT nanocomposites, which may prove to be extremely beneficial for developing microstructure in manufacturing, such as injection molding where cooling rates can exceed 600 K/s.

Declaration of competing interest

The authors declare that they have no known competing financial interests or personal relationships that could have appeared to influence the work reported in this paper.

CRediT authorship contribution statement

Anne M. Gohn: Investigation, Methodology, Writing - original draft, Writing - review & editing, Project administration. **Jiho Seo:** Formal analysis, Validation. **Ralph H. Colby:** Conceptualization, Writing - review & editing. **Richard P. Schaake:** Conceptualization, Writing - review & editing, Funding acquisition. **René Androsch:** Conceptualization, Writing - original draft, Supervision, Formal analysis. **Alicyn M. Rhoades:** Conceptualization, Supervision, Funding acquisition, Writing - review & editing.

Acknowledgments

This work was supported by the National Science Foundation under grant no. 1653629 and SKF. The authors thank Tim Tighe of the Penn State University Materials Characterization Laboratories for assistance with AFM imaging.

Appendix A. Supplementary data

Supplementary data to this article can be found online at https://doi.org/10.1016/j.polymer.2020.122548.

References

[1] A. Wang, R. Lin, C. Stark, J.H. Dumbleton, Suitability and limitations of carbon fiber reinforced PEEK composites as bearing surfaces for total joint replacements, Wear 225–229 (1999) 724–727, https://doi.org/10.1016/S0043-1648(99)00026-5.

[2] D.P. Jones, D.C. Leach, D.R. Moore, Mechanical properties of poly(ether-ether-ketone) for engineering applications, Polymer 26 (1985) 1385–1393, https://doi.org/10.1016/0032-3861(85)90316-7.

[3] J. Seo, A.M. Gohn, O. Dubin, H. Takahashi, H. Hasegawa, R. Sato, A.M. Rhoades, R. P. Schaake, R.H. Colby, Isothermal crystallization of poly(ether ether ketone) with different molecular weights over a wide temperature range, Polym. Cryst. 2 (2019), e10055, https://doi.org/10.1002/pcr2.10055.

[4] R. Androsch, A.M. Rhoades, I. Stolte, C. Schick, Density of heterogeneous and homogeneous crystal nuclei in poly (butylene terephthalate), Eur. Polym. J. 66 (2015) 180–189.

[5] A.M. Gohn, A.M. Rhoades, N. Wonderling, T. Tighe, R. Androsch, The effect of supercooling of the melt on the semicrystalline morphology of PA 66, Thermochim. Acta 655 (2017) 313–318, https://doi.org/10.1016/j.tca.2017.07.012.

[6] A. Rhoades, J. Williams, R. Androsch, Thermochimica Acta Crystallization kinetics of polyamide 66 at processing-relevant cooling conditions and high supercooling, Thermochimica Acta 603 (2015) 103–109, https://doi.org/10.1016/j.tca.2014.10.020.

[7] C. Schick, Insights into Polymer Crystallization and Melting from Fast Scanning Chip Calorimetry, 2016, p. 91, https://doi.org/10.1016/j.polymer.2016.03.038.

[8] C. Silvestre, S. Cimmino, D. Duraccio, C. Schick, Isothermal crystallization of isotactic poly (propylene) studied by superfast calorimetry, Macromol. Rapid Commun. 28 (7) (2007) 875–881.

[9] R. Androsch, C. Schick, Crystal nucleation of polymers at high supercooling of the melt, in: F. Auriemma, G.C. Alfonso, C. de Rosa (Eds.), Polymer Crystallization I From Chain Microstructure to Processing, Springer International Publishing, Cham, 2017, pp. 257–288.

[10] D.J. Blundell, B.N. Osborn, The morphology of poly (aryl-ether-ether- ketone) 24 (1983) 953–958.

[11] J.N. Coleman, U. Khan, W.J. Blau, Y.K. Gun'ko, Small but Strong: A Review of the Mechanical Properties of Carbon Nanotube-Polymer Composites, Carbon N. Y. (2006), https://doi.org/10.1016/j.carbon.2006.02.038.

[12] R. Andrews, M.C. Weisenberger, Carbon nanotube polymer composites, Current Opinion in Solid State and Materials Science 8 (1) (2004) 31–37, https://doi.org/10.1016/j.cossms.2003.10.006.

[13] Z. Spitalsky, D. Tasis, K. Papagelis, C. Galiotis, Carbon nanotube-polymer composites: chemistry, processing, mechanical and electrical properties, Prog. Polym. Sci. 35 (2010) 357–401, https://doi.org/10.1016/j.progpolymsci.2009.09.003.

[14] M.T. Byrne, Y.K. Guin'Ko, Recent advances in research on carbon nanotube - polymer composites, Adv. Mater. 22 (2010) 1672–1688, https://doi.org/10.1002/adma.200901545.

[15] R. Ramasubramaniam, J. Chen, H. Liu, Homogeneous carbon nanotube/polymer composites for electrical applications, Appl. Phys. Lett. 83 (2003) 2928–2930, https://doi.org/10.1063/1.1616976.

[16] P. Pötschke, A.R. Bhattacharyya, A. Janke, S. Pegel, A. Leonhardt, C. Täschner, M. Ritschel, S. Roth, B. Hornbostel, J. Cech, Melt mixing as method to disperse carbon nanotubes into thermoplastic polymers, Fullerenes, Nanotub. Carbon Nanostruct. 13 (2005) 211–224, https://doi.org/10.1081/FST-200039267.

[17] M.K. Seo, S.J. Park, Electrical resistivity and rheological behaviors of carbon nanotubes-filled polypropylene composites, Chem. Phys. Lett. 395 (2004) 44–48, https://doi.org/10.1016/j.cplett.2004.07.047.

[18] P. Pötschke, A.R. Bhattacharyya, A. Janke, Melt mixing of polycarbonate with multiwalled carbon nanotubes: microscopic studies on the state of dispersion, Eur. Polym. J. 40 (2004) 137–148, https://doi.org/10.1016/j.eurpolymj.2003.08.008.

[19] T. McNally, P. Pötschke, P. Halley, M. Murphy, D. Martin, S.E.J. Bell, G.P. Brennan, D. Bein, P. Lemoine, J.P. Quinn, Polyethylene multiwalled carbon nanotube composites, Polymer 46 (2005) 8222–8232, https://doi.org/10.1016/j.polymer.2005.06.094.

[20] W. Bauhofer, J.Z. Kovacs, A review and analysis of electrical percolation in carbon nanotube polymer composites, Compos. Sci. Technol. 69 (2009) 1486–1498, https://doi.org/10.1016/j.compscitech.2008.06.018.

[21] C. McClory, P. Pötschke, T. McNally, Influence of screw speed on electrical and rheological percolation of melt-mixed high-impact polystyrene/MWCNT nanocomposites, Macromol. Mater. Eng. 296 (2011) 59–69, https://doi.org/10.1002/mame.201000220.

[22] H.G. Chae, Y.H. Choi, M.L. Minus, S. Kumar, Carbon nanotube reinforced small diameter polyacrylonitrile based carbon fiber, Compos. Sci. Technol. 69 (2009) 406–413, https://doi.org/10.1016/j.compscitech.2008.11.008.

[23] W. Weng, P. Chen, S. He, X. Sun, H. Peng, Smart electronic textiles, Angew. Chem. Int. Ed. 55 (2016) 6140–6169, https://doi.org/10.1002/anie.201507333.

[24] J. Di, X. Zhang, Z. Yong, Y. Zhang, D. Li, R. Li, Q. Li, Carbon-nanotube fibers for wearable devices and smart textiles, Adv. Mater. 28 (2016) 10529–10538, https://doi.org/10.1002/adma.201601186.

[25] A. Beigbeder, P. Degee, S. Conlan, R. Mutton, A. Clare, M. Pettitt, M. Callow, Preparation and characterisation of silicone-based coatings filled with carbon nanotubes and natural sepiolite and their application as marine fouling-release coatings, Biofouling 24 (2008) 291–302.

[26] B. Zhao, J. Wang, Z. Li, P. Liu, D. Chen, Y. Zhang, Mechanical strength improvement of polypropylene threads modified by PVA/CNT composite coatings, Mater. Lett. 62 (2008) 4380–4382, https://doi.org/10.1016/j.matlet.2008.07.037.

[27] E.J. Siochi, J.S. Harrison, Structural nanocomposites for aerospace applications, MRS Bull. 40 (2015) 829–835, https://doi.org/10.1557/mrs.2015.228.

[28] S. Bellucci, C. Balasubramanian, F. Micciulla, G. Rinaldi, CNT composites for aerospace applications, J. Exp. Nanosci. 2 (2007) 193–206, https://doi.org/10.1080/17458080701376348.

[29] J. Njuguna, K. Pielichowski, Polymer nanocomposites for aerospace applications: Characterization, Adv. Eng. Mater. 6 (2004) 204–210, https://doi.org/10.1002/adem.200305110.

[30] K. Sahithi, M. Swetha, K. Ramasamy, N. Srinivasan, N. Selvamurugan, Polymeric composites containing carbon nanotubes for bone tissue engineering, Int. J. Biol. Macromol. 46 (2010) 281–283, https://doi.org/10.1016/j.ijbiomac.2010.01.006.

[31] N. Saito, Y. Usui, K. Aoki, N. Narita, M. Shimizu, K. Hara, N. Ogiwara, K. Nakamura, N. Ishigaki, H. Kato, S. Taruta, M. Endo, Carbon nanotubes: biomaterial applications, Chem. Soc. Rev. 38 (2009) 1897, https://doi.org/10.1039/b804822n. –1903.

[32] A. White, S. Best, Hydroxyapatite–carbon nanotube composites for Biomedical applications: A review, International Journal of Applied Ceramic Technology 4 (2007) 1–13.

[33] Hyperion catalysis (n.d.), (accessed June 6, 2019), http://www.hyperioncatalysis.com/technology2.htm.

[34] C. McClory, T. McNally, M. Baxendale, P. Pötschke, W. Blau, M. Ruether, Electrical and rheological percolation of PMMA/MWCNT nanocomposites as a function of CNT geometry and functionality, Eur. Polym. J. 46 (2010) 854–868, https://doi.org/10.1016/j.eurpolymj.2010.02.009.

[35] Y. Shang, X. Wu, Y. Liu, Z. Jiang, Z. Wang, Z. Jiang, H. Zhang, Preparation of PEEK/MWCNTs composites with excellent mechanical and tribological properties, High Perform. Polym. 31 (2019) 43–50, https://doi.org/10.1177/0954008317750726.

[36] A. Peigney, C. Laurent, E. Flahaut, R.R. Bacsa, A. Rousset, Specific surface area of carbon nanotubes and bundles of carbon nanotubes, Carbon 39 (4) (2001) 507–514.

[37] Y. Geng, M.Y. Liu, J. Li, X.M. Shi, J.K. Kim, Effects of surfactant treatment on mechanical and electrical properties of CNT/epoxy nanocomposites, Compos. Part A Appl. Sci. Manuf. 39 (2008) 1876–1883, https://doi.org/10.1016/j.compositesa.2008.09.009.

[38] J. Li, P.C. Ma, W.S. Chow, C.K. To, B.Z. Tang, J.K. Kim, Correlations between percolation threshold, dispersion state, and aspect ratio of carbon nanotubes, Adv. Funct. Mater. 17 (2007) 3207–3215, https://doi.org/10.1002/adfm.200700065.

[39] G.W. Lee, S. Jagannathan, H.G. Chae, M.L. Minus, S. Kumar, Carbon nanotube dispersion and exfoliation in polypropylene and structure and properties of the resulting composites, Polymer 49 (7) (2008) 1831–1840.

[40] A.R. Bhattacharyya, T. V Sreekumar, T. Liu, S. Kumar, L.M. Ericson, H. Hauge, R. E. Smalley, Crystallization and Orientation Studies in Polypropylene/Single Wall Carbon Nanotube Composite, vol. 44, 2003, pp. 2373–2377, https://doi.org/10.1016/S0032-3861(03)00073-9.

[41] L. Li, C.Y. Li, C. Ni, L. Rong, B. Hsiao, Structure and crystallization behavior of Nylon 66/multi-walled carbon nanotube nanocomposites at low carbon nanotube contents, Polymer 48 (12) (2007) 3452–3460.

[42] C. Rong, G. Ma, S. Zhang, L. Song, Z. Chen, G. Wang, P. Ajayan, Effect of carbon nanotubes on the mechanical properties and crystallization behavior of poly(ether ether ketone), Compos. Sci. Technol. 70 (2010) 380–386, https://doi.org/10.1016/j.compscitech.2009.11.024.

[43] A.M. Díez-Pascual, M. Naffakh, M.A. Gomez, C. Marco, G. Ellis, M.T. Martinez, A. Anson, J.M. Gonzalez-Dominguez, Y. Martinez-Rube, B. Simard, Development and characterization of PEEK/carbon nanotube composites, Carbon N. Y. 7 (2009) 3079–3090, https://doi.org/10.1016/j.carbon.2009.07.020.

[44] M. Kuo, J. Huang, M. Chen, Non-isothermal crystallization kinetic behavior of alumina nanoparticle filled poly(ether ether ketone), Mater. Chem. Phys. 99 (2006) 258–268, https://doi.org/10.1016/j.matchemphys.2005.10.021.

[45] B. Nazari, A.M. Rhoades, R.P. Schaake, R.H. Colby, Flow-induced crystallization of peek: Isothermal crystallization kinetics and lifetime of flow-induced precursors during isothermal annealing, ACS Macro Letters 5 (7) (2016) 849–853.

[46] T. Ogasawara, T. Tsuda, N. Takeda, Stress-strain behavior of multi-walled carbon nanotube/PEEK composites, Compos. Sci. Technol. 71 (2011) 73–78, https://doi.org/10.1016/j.compscitech.2010.10.001.

[47] M. Kalin, M. Zalaznik, S. Novak, Wear and Friction Behaviour of Poly-Ether-Ether-Ketone (PEEK) Filled with Graphene, WS2 and CNT Nanoparticles, Wear 332 (2015) 855–862, https://doi.org/10.1016/j.wear.2014.12.036.

[48] K. Könnecke, Crystallization of poly(aryl ether ketones) I. crystallization kinetics, J. Macromol. Sci. Part B. 33 (1994) 37–62, https://doi.org/10.1080/00222349408248078.

[49] V.P. Shim, J. Yuan, C.T. Lim, Dynamic tensile response of a carbon-fiber-reinforced LCP composite and its temperature sensitivity, in: Second International Conference on Experimental Mechanics, 4317, International Society for Optics and Photonics, 2001, June, pp. 100–105.

[50] F.J. Medellin-Rodriguez, P.J. Phillips, Crystallization and structure-mechanical property relations in poly(aryl ether ether ketone) [PEEK], Polym. Eng. Sci. 30 (1990) 860–869, https://doi.org/10.1002/pen.760301409.

[51] X. Tardif, B. Pignon, N. Boyard, J.W.P. Schmelzer, V. Sobotka, D. Delaunay, C. Schick, Experimental study of crystallization of PolyEtherEtherKetone (PEEK) over a large temperature range using a nano-calorimeter, Polym. Test. 36 (2014) 10–19, https://doi.org/10.1016/j.polymertesting.2014.03.013.

[52] P. Venkatraman, A.M. Gohn, A.M. Rhoades, E.J. Foster, Developing high performance PA 11/cellulose nanocomposites for industrial-scale melt processing, Compos. Part B. 174 (2019) 106988, https://doi.org/10.1016/j.compositesb.2019.106988.

[53] A. Gohn, J. Seo, T. Ferris, P. Venkatraman, E. Foster, A. Rhoades, Quiescent and flow-induced crystallization in polyamide 12/cellulose nanocrystal composites, Thermochim. Acta 667 (2019) 99–108.

[54] I. Kolesov, R. Androsch, D. Mileva, W. Lebek, A. Benhamida, M. Kaci, W. Focke, Crystallization of a polyamide 11/organo-modified montmorillonite nanocomposite at rapid cooling, Colloid Polym. Sci. 291 (11) (2013) 2541–2549.

[55] D. Mileva, A. Monami, D. Cavallo, G.C. Alfonso, G. Portale, R. Androsch, Crystallization of a polyamide 6/montmorillonite nanocomposite at rapid cooling, Macromol. Mater. Eng. 298 (9) (2013) 938–943.

[56] S. Inoue, N. Ichikuni, T. Suzuki, T. Uematsu, K. Kaneko, Capillary condensation of N 2 on multiwall carbon nanotubes, J. Phys. Chem. B 102 (2002) 4689–4692, https://doi.org/10.1021/jp973319n.

[57] A. Gohn, A. Rhoades, D. Okonski, R. Androsch, Effect of melt-memory on the crystal polymorphism in molded isotactic polypropylene, Macromol. Mater. Eng. 303 (2018), https://doi.org/10.1002/mame.201800148.

[58] E. Zhuravlev, A. Wurm, P. Pötschke, R. Androsch, J.W.P. Schmelzer, C. Schick, Kinetics of nucleation and crystallization of poly (ε -caprolactone) – multiwalled carbon nanotube composites, Eur. Polym. J. 52 (2014) 1–11, https://doi.org/10.1016/j.eurpolymj.2013.12.015.

[59] K. Jariyavidyanont, R. Androsch, C. Schick, Crystal reorganization of poly (butylene terephthalate), Polymer 124 (2017) 274–283, https://doi.org/10.1016/j.polymer.2017.07.076.

[60] J.E.K. Schawe, P. Pötschke, I. Alig, Nucleation efficiency of fillers in polymer crystallization studied by fast scanning calorimetry: carbon nanotubes in

polypropylene, Polymer 116 (2017) 160–172, https://doi.org/10.1016/j.polymer.2017.03.072.
[61] A. Nogales, T.A. Ezquerra, Z. Denchev, F.J. Baltá-Calleja, Induction time for cold crystallization in semi-rigid polymers: PEN and PEEK, Polymer 42 (2001) 5711–5715, https://doi.org/10.1016/S0032-3861(00)00929-0.
[62] A. Wurm, A. Herrmann, M. Cornelius, E. Zhuravlev, D. Pospiech, R. Nicula, C. Schick, Temperature Dependency of Nucleation Efficiency of Carbon Nanotubes in PET and PBT, 2015, pp. 637–649, https://doi.org/10.1002/mame.201400405.
[63] D.A. Ivanov, A.M. Jonas, Isothermal growth and reorganization upon heating of a single poly(aryl-ether-ether-ketone) (PEEK) spherulite, as imaged by atomic force microscopy, Macromolecules 31 (1998) 4546–4550, https://doi.org/10.1021/ma961549e.
[64] D.A. Ivanov, B. Nysten, A.M. Jonas, Atomic force microscopy imaging of single polymer spherulites during crystallization: application to a semi-crystalline blend, Polymer 40 (1999) 5899–5905, https://doi.org/10.1016/S0032-3861(98)00812-X.